IOP Publishing Journal of Optics
J. Opt. **20** (2018) 125606 (12pp) https://doi.org/10.1088/2040-8986/aaef27

Characterization of beam splitters in the calibration of a six-channel Stokes polarimeter

Song Zhang[1], Honggang Gu[1], Jiamin Liu, Hao Jiang[2], Xiuguo Chen, Chuanwei Zhang and Shiyuan Liu[2]

State Key Laboratory of Digital Manufacturing Equipment and Technology, Huazhong University of Science and Technology, Wuhan 430074, People's Republic of China

E-mail: hjiang@hust.edu.cn and shyliu@hust.edu.cn

Received 4 August 2018, revised 8 October 2018
Accepted for publication 7 November 2018
Published 22 November 2018

Abstract

Polarization distortion in a beam splitter is a phenomenon where the polarization state of output light deviates from the theoretical expectation, which is inevitable and will result in significant errors in the optical systems. A theoretical analysis method based on Mueller matrix ellipsometry is proposed for characterizing the beam splitters and the application in the calibration of a six-channel Stokes polarimeter (SP) is shown. In this study, polarization distortions in the beam splitters including depolarization, linear birefringence, circular birefringence, linear dichroism, and circular dichroism have been considered. With the proposed method, the beam splitters are characterized by the polarization distortions and the effective optical parameters extracted. In our experiment, the Mueller matrices of two different commonly used beam splitters measured by a commercial Mueller matrix ellipsometer (MME) are consistently fitted by the proposed method and the residual errors have shown improvement compared to the conventional methods. A practical application of the proposed method is exhibited by calibrating a SP system containing two non-polarization beam splitters and three polarization beam splitters. With the proposed method introduced, the general error of the measured Stokes vector can be reduced from 3% to 1%, and the errors of the thickness measurement of standard SiO_2 thin film samples are within 1 nm compared with the results reported by a commercial MME.

Keywords: beam splitter, polarization distortion, Stokes polarimeter, characterization, calibration

(Some figures may appear in colour only in the online journal)

1. Introduction

Beam splitters are one of the most critical optical components in a splitting optical system, which can be mainly divided into two categories: polarization beam splitter (PBS), and non-PBS (NPBS). An ideal PBS can separate the s-component from the p-component in the incident light [1], while an ideal NPBS can divide the incident light into two beams with a specific intensity ratios [2]. Since no mechanical movement or other optoelectronic modulation is introduced, beam splitters act as critical roles in many optical systems, especially in the systems emphasizing the temporal resolution. However, due to the inevitable polarization distortion in a beam splitter, the ideal working conditions are impossible to achieve. Therefore, it is of great importance to accurately characterize the beam splitters as well as to calibrate the systems delicately.

In recent years, many researchers have been engaged in compensating or characterizing the polarization distortions in beam splitters. Azzam used the ellipsometric parameters to characterize the NPBS in the division-of-amplitude photopolarimeter, in which the application is not suitable for an

[1] These authors contributed equally to this work.
[2] Authors to whom any correspondence should be addressed.

optical anisotropy interface of an actual beam splitter [3, 4]. In the retardance measurement with an interferometric ellipsometer, Lysenko *et al* characterized the NPBS with the amplitude coefficients of transmission and reflection by using the Jones matrix formalism [5]. Liu *et al* proposed a composite optical structure consisting of two quarter-wave plates and a half-wave plate to compensate the polarization distortion induced by a non-ideal NPBS in a Michelson interferometer. Although the linear birefringence (LB) and circular birefringence (CB) of the polarization distortion can be compensated well, the other remaining polarization distortions are not taken into consideration [6], which may significantly degrade the measurement accuracy. Pezzaniti *et al* proposed a method for PBS characterization in terms of its diattenuation, optical rotation and phase retardance with Mueller matrix in 1994. Unfortunately, the depolarization (Dep) and circular dichroism (CD), which may play more critical roles in polarization-selective devices, such as PBS, are not discussed as well [7]. Tyan *et al* used several parameters, such as the polarization extinction ratio, reflectivity and transmittance of the s- and the p-component of the incident light, to describe the PBS in the numerical simulation based on effective-medium theory and rigorous coupled-wave analysis [8]. In addition to the parameters achieved using Tyan's method, the frustrated total internal reflection method proposed by Li *et al* can extract the phase changes, while the other polarization distortions are not mentioned [9]. Since all of the characterization methods mentioned above can only partially characterize the polarization distortion of a beam splitter, it is highly desirable to develop a general method to characterize the beam splitters accurately for polarizing optical instrumentation.

With the advantages of high temporal resolution, high accuracy and good stability, the Stokes polarimeter (SP) has been widely used in many areas, such as astronomy [10–12], remote sensing [13, 14] and material characterization [15, 16]. Among the existing techniques, the SP based on the spatial division of amplitude is a typical configuration, which employs multiple NPBSs and PBSs in the optical paths [17]. Therefore, the measurement accuracy of such an optical system heavily depends on the characterization and *in situ* calibration of the beam splitters [18], which has already attracted comprehensive attention in past literature.

In 1981, Azzam used reference lights with four different known polarization states to calibrate a division-of-amplitude polarimeter. The calibration procedure based on overall instrument matrix makes it unnecessary to know the properties of individual components in the polarimeter. Since the reference lights act as standard inputs, the accuracy of the polarimeter heavily depends on the selections of the reference lights [19]. Boulbry *et al* calibrated a SP by using a set of well-characterized reference polarization states. The calibration method reduces the effect of statistical sources of noise on the precision with the method of singular value decomposition. However, it is usually challenging to achieve the well-characterized reference polarization states [20]. Although the eigenvalue calibration method introduced by Compain *et al* is optical element independent and no first order approximations are made, the accuracy of the calibrated instrument heavily depends on the characteristics of the reference samples [21]. In a word, the calibration methods mentioned above avoid the error caused by polarization distortion in the beam splitters, but their application range is limited.

In this work, a beam splitter characterization method using Mueller matrix ellipsometry is proposed first. Then, a six-channel SP which employs two NPBSs and three PBSs has been developed, with the corresponding calibration method combined with the characterization method being applied. In the proposed characterization model, beam splitter polarization distortion is described by several effective optical parameters. By comparing with the conventional characterization methods, significant improvement can be read from the decreased residual fitting errors of Mueller matrix elements. Compared to the measured thickness results of a set of standard SiO_2 thin films given by a commercial Mueller matrix ellipsometer (MME), the deviations within 1 nm demonstrate the accuracy of the calibrated SP as well as the effectiveness of the proposed methods.

2. Characterization of beam splitters

The polarization state of the light passing through the optical elements may deviate from the theoretical expectation. In general, such polarization distortion is inevitable due to the design and manufacturing defects, as well as the unsatisfactory installations. The polarization distortions of a beam splitter mainly include Dep, LB, CB, linear dichroism (LD) and CD. Among these properties, the CB is usually affected by the installation conditions of the beam splitters, while the LB and Dep are typically resulted from the inhomogeneous interface in the beam splitters. Besides, the LD and CD are properties which determine the transmittance or absorption according to the polarization state of light.

According to the designed function, beam splitters can be mainly divided into two categories, NPBS and PBS. An ideal NPBS can be considered as an ideal free-space medium which can divide the incident light into two beams with a specific intensity ratio. Meanwhile an ideal PBS can filter out the s-component in the transmitted branch or filter out the p-component in the reflected branch, which is similar to a linear polarizer. In order to fully characterize the polarization distortion of an imperfect beam splitter, all of the Dep, LB, LD, CB and CD should be considered in the beam splitters characterization, as shown in figure 1. It should be noted that the characterization method is suitable for reflection and transmission of beam splitters with different types.

According to figure 1, the characterization of a beam splitter using Mueller matrix can be expressed as

$$\mathbf{M}_{\mathrm{BS}} = \mathbf{M}_{\mathrm{Dep}}\mathbf{M}_{\mathrm{LD}}\mathbf{M}_{\mathrm{LB}}\mathbf{M}_{\mathrm{CD}}\mathbf{M}_{\mathrm{CB}}\mathbf{M}_{\mathrm{Fm}}, \tag{1}$$

where the Mueller matrix of an ideal free medium is given in equation (2). In addition, the '+' is for the transmission

matrix and '−' is for the reflection matrix [22]

$$\mathbf{M}_{\mathrm{Fm}} = \begin{bmatrix} 1 & 0 & 0 & 0 \\ 0 & 1 & 0 & 0 \\ 0 & 0 & \pm 1 & 0 \\ 0 & 0 & 0 & \pm 1 \end{bmatrix}. \tag{2}$$

The Mueller matrix of a device with LB properties such as a wave plate or a retarder with a fast axis at β and a retardance δ [23] can be expressed as

$$\mathbf{M}_{\mathrm{LB}} = \begin{pmatrix} 1 & 0 & 0 & 0 \\ 0 & \cos(4\beta)\sin(\delta/2)^2 + \cos(\delta/2)^2 & \sin(4\beta)\sin(\delta/2)^2 & -\sin(2\beta)\sin(\delta) \\ 0 & -\sin(4\beta)\sin(\delta/2)^2 & -\cos(4\beta)\sin(\delta/2)^2 + \cos(\delta/2)^2 & \cos(2\beta)\sin(\delta) \\ 0 & \sin(4\beta)\sin(\delta/2)^2 & -\cos(2\beta)\sin(\delta) & \cos(\delta) \end{pmatrix}. \tag{3}$$

Meanwhile, the Mueller matrix for a device with LD properties, which has a diattenuation axis angle θ_{d} and diattenuation D [24], has the expression as equation (4).

$$\mathbf{M}_{\mathrm{LD}} = \begin{pmatrix} 1 & -D\cos(2\theta_{\mathrm{d}}) & -D\sin(2\theta_{\mathrm{d}}) & 0 \\ -D\cos(2\theta_{\mathrm{d}}) & \cos(2\theta_{\mathrm{d}})^2 + 2\sin(2\theta_{\mathrm{d}})^2\sqrt{1-D^2} & \cos(2\theta_{\mathrm{d}})\sin(2\theta_{\mathrm{d}})(1-2\sqrt{1-D^2}) & 0 \\ -D\sin(2\theta_{\mathrm{d}}) & \cos(2\theta_{\mathrm{d}})\sin(2\theta_{\mathrm{d}})(1-2\sqrt{1-D^2}) & \sin(2\theta_{\mathrm{d}})^2 + 2\cos(2\theta_{\mathrm{d}})^2\sqrt{1-D^2} & 0 \\ 0 & 0 & 0 & 2\sqrt{1-D^2} \end{pmatrix}. \tag{4}$$

As described in [25, 26], the Mueller matrix for a device with CB properties such as optically active material with an optical rotation angle γ can be written as equation (5)

$$\mathbf{M}_{\mathrm{CB}} = \begin{pmatrix} 1 & 0 & 0 & 0 \\ 0 & \cos(2\gamma) & \sin(2\gamma) & 0 \\ 0 & -\sin(2\gamma) & \cos(2\gamma) & 0 \\ 0 & 0 & 0 & 1 \end{pmatrix}. \tag{5}$$

Besides the above, the Mueller matrix for a device with CD properties that the circular amplitude anisotropy is R [27] can be expressed as equation (6)

$$\mathbf{M}_{\mathrm{CD}} = \begin{pmatrix} 1 & 0 & 0 & 2R/(1+R^2) \\ 0 & (1-R^2)/(1+R^2) & 0 & 0 \\ 0 & 0 & (1-R^2)/(1+R^2) & 0 \\ 2R/(1+R^2) & 0 & 0 & 1 \end{pmatrix}. \tag{6}$$

Finally, the Mueller matrix describing the depolarization effect [27–29] can be written as

$$\mathbf{M}_{\mathrm{Dep}} = \begin{pmatrix} 1 & p_1 & p_2 & p_3 \\ p_1 & e_1 & -p_4 & -p_5 \\ p_2 & p_4 & e_2 & -p_6 \\ p_3 & p_5 & p_6 & e_3 \end{pmatrix}, \tag{7}$$

where e_1 and e_2 are the degrees of linear depolarization, and e_3 is the degree of circular depolarization. Meanwhile, the e_1, e_2 and e_3 can be set as 0.99 according to the multiple repeated experiments. To simplify the analytical model and reduce the parameters of modeling, the Mueller matrix of depolarization properties for a PBS can be rewritten as equation (8*a*), while as equation (8*b*) for an NPBS, according to their perspective depolarization characteristics,

$$\mathbf{M}_{\mathrm{Dep\_P}} = \begin{pmatrix} 1 & 0 & 0 & p_3 \\ 0 & e_1 & 0 & p_3 \\ 0 & 0 & e_2 & 0 \\ p_3 & -p_3 & 0 & e_3 \end{pmatrix}, \tag{8a}$$

$$\mathbf{M}_{\mathrm{Dep\_NP}} = \begin{pmatrix} 1 & p_1 & 0 & 0 \\ p_1 & e_1 & 0 & -p_5 \\ 0 & 0 & e_2 & 0 \\ 0 & p_5 & 0 & e_3 \end{pmatrix}. \tag{8b}$$

The depolarization index DI can be introduced to quantify the degree of depolarization, by which 1 stands for

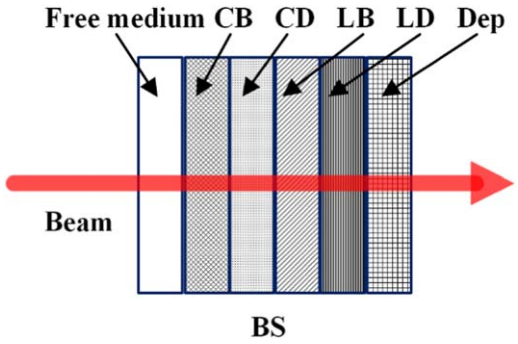

Figure 1. Schematic illustration of beam splitters with LB, LD, CB, CD and Dep.

a non-depolarization device, and 0 represents an ideal depolarizer. The depolarization index DI [30] can be defined as equation (9)

$$\mathrm{DI}[\mathbf{M}] = \frac{\sqrt{\sum_{i,j=0}^{3} m_{ij}^2 - m_{00}^2}}{\sqrt{3}\, m_{00}}. \tag{9}$$

In the end, what needs additional explanation is that β and θ_{d} are usually around 0 and have a minor effect on the final results. Therefore, they can be set as 0 to simplify the model and reduce the parameters in the calibration. The proposed method enables a decoupled extraction of the relative optical parameters in the defined range. It is noted that equations (3)–(8) yield values of δ, D, R, γ, p_1, p_3 and p_5 in the ranges $-180^\circ \leqslant \delta \leqslant 180^\circ$, $-1 \leqslant D \leqslant 1$, $-1 \leqslant R \leqslant 1$, $0 \leqslant \gamma \leqslant 180^\circ$ and $-1 \leqslant p_1,\ p_3,\ p_5 \leqslant 1$, respectively.

3. Instrument and principle of calibration

Based on the spatial division of amplitude method, a SP with six parallel detection channels is developed to measure the instantaneous changes of optical constants during rapid processes. As schematically shown in figure 2(a), the SP consists of three parts: a polarization state generator (PSG), a sample stage and a fast polarization measurement system (FPMS). The PSG consists of a 5 mW Red (632.8 nm) He–Ne Laser (THORLABS), two linear polarizers and a zero-order quarter-wave plate. Since the laser source produces a linear polarized light, the first polarizer acts as an attenuator to adjust the light intensity to a suitable range. Then, the polarization state of the probing beam is changed by the second polarizer which acts as a polarization generator. Besides, the quarter-wave plate inserted between the two polarizers changes the linear polarized light into the right-circular polarized light to avoid the extinction effect caused by the different azimuth angles of the two polarizers. The sample stage consists of a dovetail translational stage and a tilt platform to adjust the posture of the sample under different measurement configurations. The FPMS is composed of two NPBSs with split ratios of 7:3 (R:T) and 5:5 (R:T), respectively, a quart-wave plate, a half-wave plate, three PBSs and six photomultiplier tubes (PMT). The polarimeter is mounted on a rotatable base so that it can be used in both transmissive mode, and reflective mode with multi-incident angles.

In general, the calibration is divided into two steps:

(1) The fast axes of the linear polarizers and wave plates and the retardances of the wave plates in the specific azimuth are measured by a commercial MME in advance. The linear polarizer $\mathrm{P_1}$ and wave plates are mounted on a precision rotation mount and fixed at a specific azimuth, as shown in figure 3.

(2) The polarization state of the incident light is continuously modulated by the linear polarizer $\mathrm{P_2}$ which is mounted on a motorized rotation stage. Then, the incident light enters the FPMS after being reflected by the surface of the sample. Finally, the effective optical parameters of the PBSs and NPBSs can be extracted from the continuously varying light intensity based on a least-squares fitting algorithm using the principle of calibration.

Next, the principle of calibration to extract the effective optical parameters of beam splitters and the Stokes vectors of the output light will be proposed here. Without loss of generality, the polarization state of the source laser can be assumed as $\mathbf{S}_{\mathrm{laser}} = [1,\ 1,\ 0,\ 0]^{\mathrm{T}}$. Then, the Stokes vector of the output light can be expressed in a Stokes–Mueller formalism [31] shown as

$$\begin{aligned}\mathbf{S}_{\mathrm{out}} = {} & \mathbf{M}_{\mathrm{S}}[\mathbf{R}(-\theta_2)\mathbf{M}_{\mathrm{p_2}}\mathbf{R}(\theta_2)][\mathbf{R}(-\alpha_1)\mathbf{M}_{\mathrm{C_1}}\mathbf{R}(\alpha_1)] \\ & \times [\mathbf{R}(-\theta_1)\mathbf{M}_{\mathrm{p_1}}\mathbf{R}(\theta_1)]\mathbf{S}_{\mathrm{laser}},\end{aligned} \tag{10}$$

where $\mathbf{M}_{\mathrm{s}}$ is the Mueller matrix of the sample, $\mathbf{M}_i$ ($I = \mathrm{P_1}, \mathrm{C_1}, \mathrm{P_2}$) represent the Mueller matrices of the corresponding optics, and $\mathbf{R}(x)$ ($x = \alpha_1,\ \theta_1,\ \theta_2$) is the Mueller rotation transformation matrix in which x is the azimuth angle of the optics axis in the polarized elements. It is noted that α_1 is the azimuth of the wave plates $\mathrm{C_1}$, θ_1 and θ_2 are the azimuth of the linear polarizers $\mathrm{P_1}$ and $\mathrm{P_2}$. In addition, the θ_1 and α_1 are set as 0° and 45° to avoid extinction.

In the FPMS, according to the definition of Stokes vector, the two NPBSs divide the output light into three branches. The first branch is demodulated by a PBS to get the Stokes vector component S_1 ($S_1 = I_x - I_y$). The second branch is demodulated by a half-wave plate and a PBS to get the Stokes vector component S_2 ($S_2 = I_{+45^\circ} - I_{-45^\circ}$). The third branch is demodulated by a quart-wave plate and a PBS to get the Stokes vector component S_3 ($S_3 = I_r - I_l$). After the demodulation, the output light is eventually divided into six sub-beams and detected by six PMT. The first Stokes vector component S_1 can be achieved from the linear relationship with light intensity [22]. The measured light intensity I_j (j = 1–6) can be written as

$$I_1 = k_1 \cdot [1 \quad 0 \quad 0 \quad 0]^{\mathrm{T}} \cdot \mathbf{\Lambda}_{\mathrm{PBS}} \cdot \mathbf{\Gamma}_{\mathrm{NPBS55}} \cdot \mathbf{\Lambda}_{\mathrm{NPBS73}} \cdot \mathbf{S}_{\mathrm{out}}, \tag{11a}$$

$$I_2 = k_2 \cdot [1 \quad 0 \quad 0 \quad 0]^{\mathrm{T}} \cdot \mathbf{\Gamma}_{\mathrm{PBS}} \cdot \mathbf{\Gamma}_{\mathrm{NPBS55}} \cdot \mathbf{\Lambda}_{\mathrm{NPBS73}} \cdot \mathbf{S}_{\mathrm{out}}, \tag{11b}$$

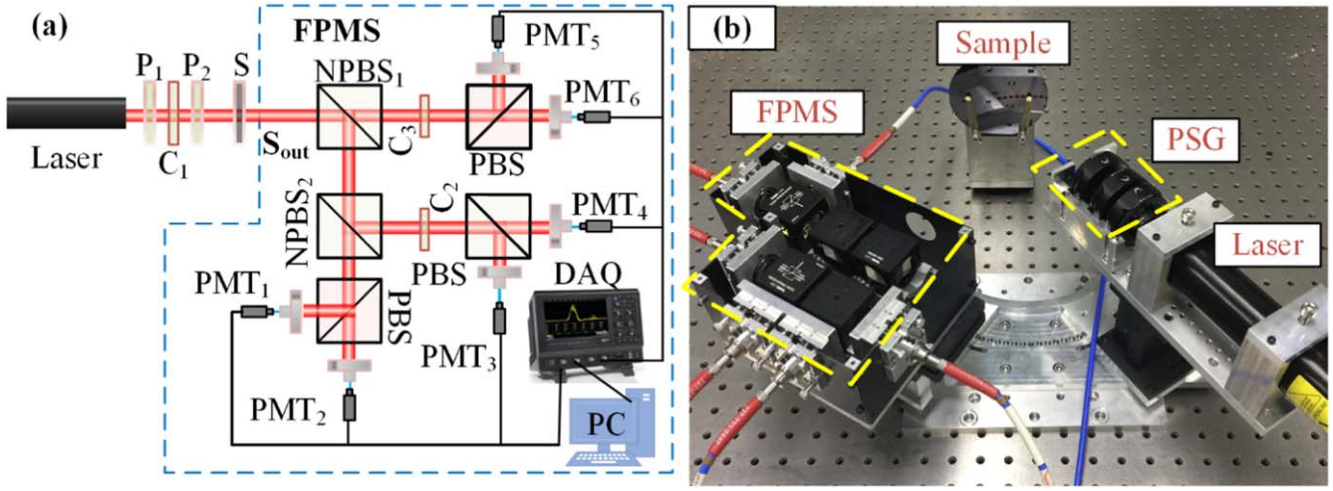

Figure 2. A six-channel Stokes polarimeter: (a) light path diagram: P_1 and P_2—polarimeter; C_1 and C_3—quart-wave plate; S—sample; C_2—half-wave plate; $NPBS_1$—70:30 (*R*:*T*) NPBS; $NPBS_2$—50:50 (*R*:*T*) NPBS; DAQ—oscilloscope; PC—personal computer; (b) house-developed instrument prototype.

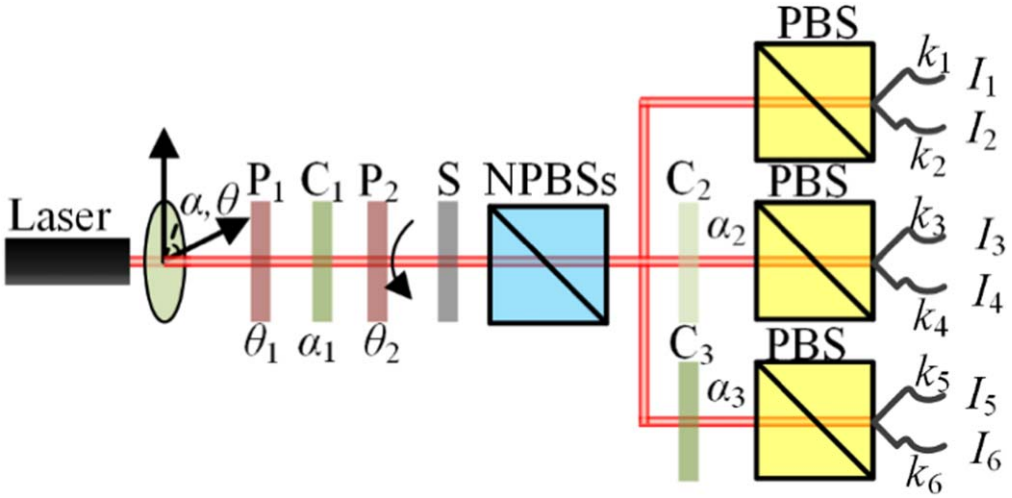

Figure 3. Instrument calibration diagram: θ_1 is fixed at 0° which is the azimuth of polarizer P_1; θ_2 is variable which is the azimuth of polarizer P_2; α_1 is fixed at 45° which is the azimuth of polarizer C_1; α_2 is fixed at 22.5° which is the azimuth of half-wave plate C_2; α_3 is fixed at 45° which is the azimuth of quart-wave plate C_3; NPBSs are the combination of the 70:30 (*R*:*T*) NPBS and 50:50 (*R*:*T*) NPBS; k_i (i = 1–6) is photoelectric conversion gain coefficient; I_j (j = 1–6) is the intensity measured by the six photomultiplier tubes; S is a well-characterized SiO_2 thin film sample.

$$I_3 = k_3 \cdot [1 \quad 0 \quad 0 \quad 0]^{\mathrm{T}} \cdot \mathbf{\Lambda}_{\mathrm{PBS}} \cdot [\mathbf{R}(-\alpha_2) \cdot \mathbf{M}_{\mathrm{C_2}} \cdot \mathbf{R}(\alpha_2)] \cdot \mathbf{\Lambda}_{\mathrm{NPBS55}} \cdot \mathbf{\Lambda}_{\mathrm{NPBS73}} \cdot \mathbf{S}_{\mathrm{out}}, \tag{11c}$$

$$I_4 = k_4 \cdot [1 \quad 0 \quad 0 \quad 0]^{\mathrm{T}} \cdot \mathbf{\Gamma}_{\mathrm{PBS}} \cdot [\mathbf{R}(-\alpha_2) \cdot \mathbf{M}_{\mathrm{C_2}} \cdot \mathbf{R}(\alpha_2)] \cdot \mathbf{\Lambda}_{\mathrm{NPBS55}} \cdot \mathbf{\Lambda}_{\mathrm{NPBS73}} \cdot \mathbf{S}_{\mathrm{out}}, \tag{11d}$$

$$I_5 = k_5 \cdot [1 \quad 0 \quad 0 \quad 0]^{\mathrm{T}} \cdot \mathbf{\Lambda}_{\mathrm{PBS}} \cdot [\mathbf{R}(-\alpha_3) \cdot \mathbf{M}_{\mathrm{C_3}} \cdot \mathbf{R}(\alpha_3)] \cdot \mathbf{\Gamma}_{\mathrm{NPBS73}} \cdot \mathbf{S}_{\mathrm{out}}, \tag{11e}$$

$$I_6 = k_6 \cdot [1 \quad 0 \quad 0 \quad 0]^{\mathrm{T}} \cdot \mathbf{\Gamma}_{\mathrm{PBS}} \cdot [\mathbf{R}(-\alpha_3) \cdot \mathbf{M}_{\mathrm{C_3}} \cdot \mathbf{R}(\alpha_3)] \cdot \mathbf{\Gamma}_{\mathrm{NPBS73}} \cdot \mathbf{S}_{\mathrm{out}}, \tag{11f}$$

where k_j (j = 1–6) is photoelectric conversion gain coefficient; $\mathbf{\Lambda}$ and $\mathbf{\Gamma}$ represent the reflection matrix and the transmission matrix, respectively; $\mathbf{M}_i$ (i = C_2, C_3, PBS, NPBS73, NPBS55) is the Mueller matrix of corresponding optical elements. Additionally, α_2 and α_3 are set as 22.5° and 45° which are the azimuth of the wave plates C_2 and C_3.

It should be noted that the three PBSs are assumed identical in calibration. Although it is better to calibrate the three beam splitters separately in order to further improve the accuracy of the polarizer. Practically, since the three PBSs are

Table 1. Optical parameters extracted from Mueller matrices of PBS and NPBS measured by MME.[a]

Beam splitters	Optical parameters		Beam splitters	Optical parameters	
PBS (*R*)	δ	−0.1000°	50:50 (*R*:*T*) NPBS (*R*)	δ	−39.45°
	D	0.9981		*R*	0.0002
	R	−0.0367		γ	−0.0904°
	γ	0.4240°		p_1	−0.0207
	p_3	0.0082		p_5	−0.0109
	DI[**M**]	0.9900		*D*	0.0001
				DI[**M**]	0.9902
PBS (*T*)	δ	−0.5730°	50:50 (*R*:*T*) NPBS (*T*)	δ	14.52°
	D	−1.000		*R*	−0.0001
	R	−0.043		γ	−0.0034°
	γ	0.0688°		p_1	−0.0065
	p_3	0.0127		p_5	−0.0029
	DI[**M**]	0.9901		*D*	0.0003
				DI[**M**]	0.9900

[a] The effective optical parameters δ is the retardance of LB property; *D* is the diattenuation of LD property; *R* is the circular amplitude anisotropy of CD property; γ is the optical rotation angle of CB property; p_1, p_3 and p_5 are the depolarization parameters; DI[**M**] is the depolarization index.

from the same manufacturer and have been mounted on the same tilt platform to ensure the same installation status, the differences in the optical parameters of the PBSs measured by the commercial MME are less than 0.005. We believe the differences among the PBSs play a small impact on the measurement results in the current accuracy. Besides, compared with the improved accuracy of the separate calibration, the difficulty and the instability of the fitting due to the increase of parameter numbers are more significant.

In particular, to disentangle the combined effects of the NPBS, PBS and wave plates, a pre-calibration process has been carried out using a commercial MME. Before the *in situ* calibration of the beam splitters, the fast axes and retardances of the wave plates and the Mueller matrices of the beam splitters are measured by the commercial MME in advance. Such a procedure is necessary for two reasons. The first one is to provide a good initial value for *in situ* calibration of beam splitters, and the other is to precisely adjust the azimuths of the wave plates to the angles required in the calibration experiment. As we have known, the polarization transmission characteristic of the optical system can be expressed by matrices multiplication of the optical elements. When the forms of the matrices and the order of the multiplication are determined, the optical parameter values of the optical elements becomes unique. Meanwhile, the forms of the optical elements metrices and the order of the multiplication are proposed uniquely in the principle of the calibration. So, the disentanglement of the combined effects of the wave plates and the beam splitters is good enough when the initial value is good in the fitting process.

The instrument matrix of the FPMS $\mathbf{M}_{\mathrm{FPMS}}$ can be modified as equation (12)

$$\mathbf{I} = \left[\frac{I_1}{k_1}\ \frac{I_2}{k_2}\ \frac{I_3}{k_3}\ \frac{I_4}{k_4}\ \frac{I_5}{k_5}\ \frac{I_6}{k_6}\right]^{\mathrm{T}} = \mathbf{M}_{\mathrm{FPMS}}\mathbf{S}_{\mathrm{out}}. \tag{12}$$

The Stokes vector of the output light $\mathbf{S}_{\mathrm{meas}}$ in each measurement can be calculated using equation (13)

$$\mathbf{S}_{\mathrm{meas}} = (\mathbf{M}_{\mathrm{FPMS}}^{\mathrm{T}}\mathbf{M}_{\mathrm{FPMS}})^{-1}\mathbf{M}_{\mathrm{FPMS}}^{\mathrm{T}}\mathbf{I}. \tag{13}$$

If the incident light is a linear polarized light oriented at 45°, the ellipsometry angles (ψ, Δ) can be calculated from the Stokes vector components [32] using

$$\psi = \frac{1}{2}\cos^{-1}\left(\frac{-S_1}{S_0}\right), \tag{14a}$$

$$\Delta = \begin{cases} \tan^{-1}(-S_3/S_2) & \text{for } \cos\Delta > 0, \\ \tan^{-1}(-S_3/S_2) + 180^\circ & \text{for } \cos\Delta < 0, \ \sin\Delta \geqslant 0, \\ \tan^{-1}(-S_3/S_2) - 180^\circ & \text{for } \cos\Delta < 0, \ \sin\Delta < 0. \end{cases} \tag{14b}$$

Then, the optical properties of the sample such as film thickness and refractive index can be calculated with the ellipsometric angles.

4. Experimental measurements and results

In this section, the validity of the characterization method will be evaluated by reconstructing the Mueller matrices of beam splitters using the effective optical parameters extracted and comparing the achieved residual errors to those using conventional methods. Further, the feasibility and effectiveness of applying the proposed characterization model in the calibration of the SP are demonstrated by the experiments on a set of standard SiO_2 thin films with different thicknesses.

As an example, we have measured the transmission and reflection Mueller matrices of a cubic PBS, and a 50:50 (*R*:*T*) cubic NPBS (Thorlabs Co, Ltd) with a commercial broadband MME (ME-L, Wuhan Eoptics Technology Co, Ltd). The MME has a composite light source (xenon lamp and halogen lamp) and the spectral range is from 200 to 1000 nm.

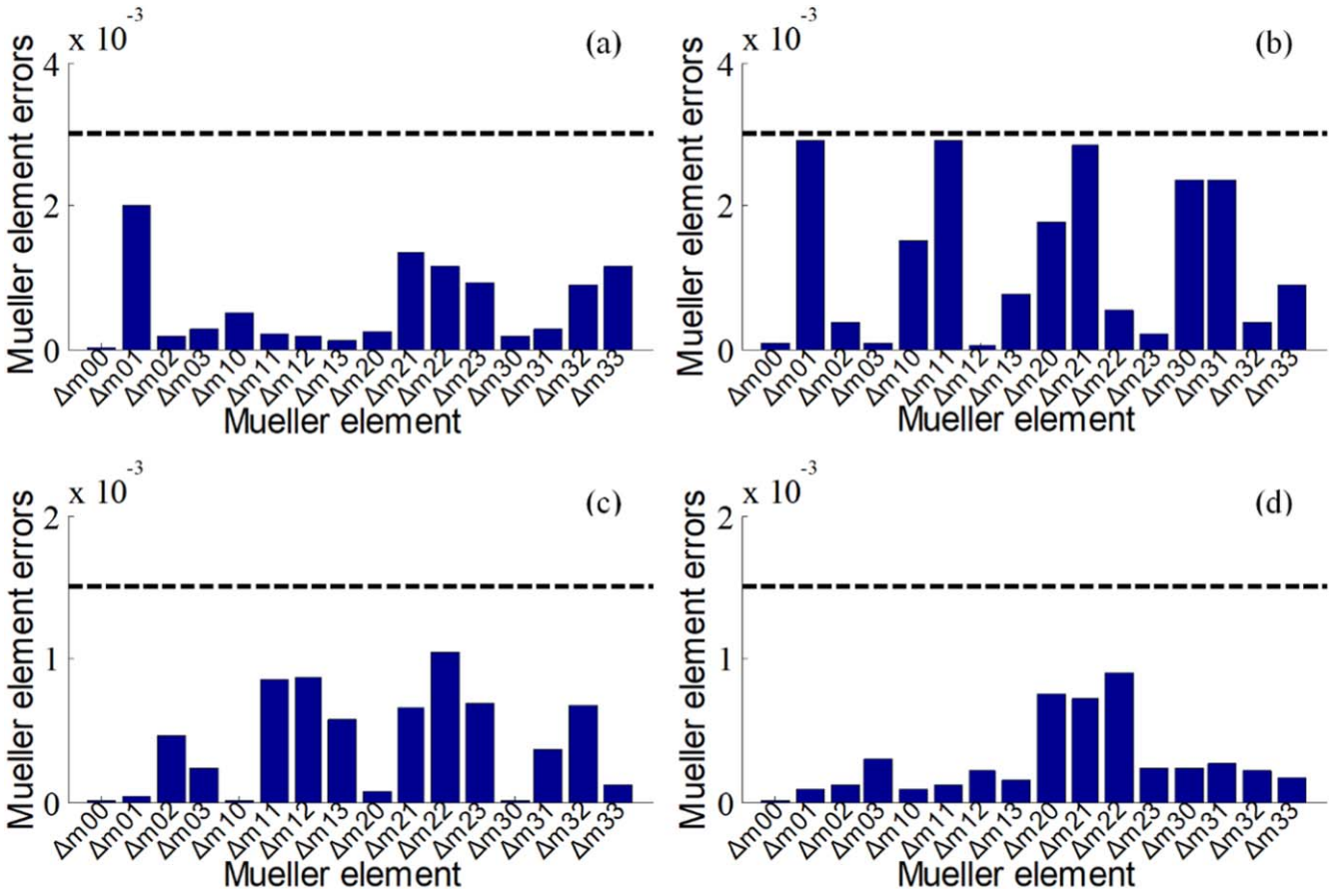

Figure 4. Residual errors in Mueller elements for (a) transmission of PBS; (b) reflection of PBS; (c) transmission of 50:50 (*R*:*T*) NPBS; (d) reflection of 50:50 (*R*:*T*) NPBS.

Table 2. Er_{ave} of Mueller matrix between different methods.

	Methods	
Beam splitters	Proposed method	Conventional method
PBS (*T*)	9.25×10^{-4}	3.17×10^{-2}
PBS (*R*)	1.65×10^{-3}	4.86×10^{-2}
50:50 (*R*:*T*) NPBS (*T*)	5.25×10^{-4}	2.45×10^{-3}
50:50 (*R*:*T*) NPBS (*R*)	3.75×10^{-4}	7.98×10^{-3}

Moreover, the MME with a dual rotating-compensator configuration can obtained the full Mueller matrix elements in a single measurement. The effective optical parameters were extracted from the measured Mueller matrices based on a least-squares fitting algorithm using the proposed characterization model. The extracted optical parameters are shown in table 1.

According to the design objective of a beam splitter, the retardance δ is expected to be around 0°. As shown in table 1, we can observe that the retardance δ is around 0° for the PBS while not for the NPBS. The retardance deviation of the NPBS is mainly due to the different absorptions and phase shifts of s- and p-components because of the broadband design of the coating. Due to the characteristic of polarization selection, the CD and LD properties of the PBS are much more pronounced than those of the NPBS. The effective optical parameters *R* and *D* are almost 0 in the calibration of the NPBSs. So, CD and LD can be eliminated in the characterization of the NPBS to simplify the fitting process under the normal condition. The Dep and CB properties usually depend on the location of the measurement as well as the installation conditions. Therefore, the non-negligible Dep and CB properties may vary in each measurement.

With the effective optical parameters shown in table 1, we can calculate the fitting Mueller matrices of the beam splitters using the proposed characterization model. To evaluate the performance of the proposed method, the residual errors defined as equation (15) are shown in figure 4.

$$\Delta m_{ij} = m_{ij}^{\mathrm{f}} - m_{ij}^{\mathrm{m}}, \tag{15}$$

where m_{ij}^{f} and m_{ij}^{m} (i, j = 0–3) are the *i*th row and *j*th column elements of the fitting and the measured Mueller matrices, respectively.

As shown in figures 4(a) and (b), for the PBS, the residual errors in Mueller matrix elements are all below 3×10^{-3}, while 1.5×10^{-3} for the NPBS, as shown in figures 4(c) and (d). It is a good embodiment of the excellent performance that the measured Muller matrices are consistently fitted by the proposed method.

As mentioned in section 1, only the LB and CB are compensated in the characterization of the NPBS and LB, LD and CB are included in the characterization of the PBS using

Table 3. Optical parameters extracted from Mueller matrices of PBS and NPBS in the *in situ* calibration.[a]

Beam splitters	Optical parameters		Beam splitters	Optical parameters	
PBS (*R*)	δ	−0.10°	50:50 (*R*:*T*) NPBS (*R*)	δ	−43.44°
	D	1.000		*R*	0.0067
	R	−0.0005		γ	−0.7888°
	γ	−0.5402°		p_1	−0.0155
	p_3	0.0094		p_5	0.1501
	DI[**M**]	0.9901		*D*	0.0010
				DI[**M**]	0.9976
PBS (*T*)	δ	−0.5730°	50:50 (*R*:*T*) NPBS (*T*)	δ	14.07°
	D	−0.9969		*R*	−0.0008
	R	−0.0033		γ	−7.2462°
	γ	0.2670°		p_1	−0.0043
	p_3	0.0130		p_5	0.0726
	DI[**M**]	0.9901		*D*	0.0005
				DI[**M**]	0.9918

[a] The effective optical parameters δ is the retardance of LB property; *D* is the diattenuation of LD property; *R* is the circular amplitude anisotropy of CD property; γ is the optical rotation angle of CB property; p_1, p_3 and p_5 are the depolarization parameters; DI[**M**] is the depolarization index.

the conventional characterization methods. In contrast, the characterization method proposed in this paper takes full account of all polarization distortions in the beam splitters. Then, a significant improvement of the proposed method can be further exhibited by employing the average residual errors Er_{ave} quantified by carrying out a comparison of the deviation of Mueller matrix formulated as equation (16) with the conventional method [6, 7], as shown in table 2

$$Er_{ave} = \sqrt{\frac{\sum_{i=0}^{3}\sum_{j=0}^{3}\Delta m_{ij}^2}{16}}. \tag{16}$$

As shown in table 2, the Er_{ave} is below 2×10^{-3} for PBS, while 6×10^{-4} for NPBS. Meanwhile, the Er_{ave} of the Mueller matrix fitted by the proposed method is much smaller than that fitted by conventional method. The much more significant improvement on PBS fitting indicates that the CD is an indispensable property in characterizing optical elements with polarization-selective properties, which is usually ignored in the existing methods.

Then, we apply the proposed characterization model to perform the *in situ* calibration of beam splitters in the house-developed SP mentioned in section 3. In the SP system, five beam splitters are used, including 3 PBSs, one 50:50 (*R*:*T*) NPBS and one 70:30 (*R*:*T*) NPBS. The Mueller matrices of these beam splitters are calibrated *in situ* using the proposed method and the extracted optical parameters are given in table 3. For the convenience of comparison with the fitting results, only the data of one PBS and the 50:50 (*R*:*T*) NPBS are list here.

Compared with the effective optical parameters shown in table 1, the difference is mainly focused on the Dep and CB, because of the different installations and locations of the splitters in the measurement. According to [7], if the skew problem of the beam splitter can be reduced to a one-dimensional problem, there is a linear relationship between the tilt angle ϕ and the optical parameter γ as expressed by

$$\phi = \frac{\gamma}{n_c}, \tag{17}$$

where n_c is refractive index of cube. In a word, the different installation states can be manifested by the difference in the CB property.

If the difference of the installation is compensated, i.e. the optical parameter γ of CB is compensated, the depolarization will be the most significant reason for the difference between the compensated Mueller matrices and measured Mueller matrices. Thus, the Mueller matrices of the beam splitters can then be expressed as

$$\mathbf{M}_{\mathrm{NPR}}^{\mathrm{cc}} = \begin{pmatrix} 1.0000 & -0.0125 & -0.0092 & -0.0097 \\ -0.0145 & 0.9989 & 0.1055 & 0.1068 \\ -0.0000 & 0.0032 & -0.7250 & 0.6871 \\ 0.0135 & 0.1499 & -0.6868 & -0.7254 \end{pmatrix},$$
$$\mathbf{M}_{\mathrm{NPR}}^{\mathrm{m}} = \begin{pmatrix} 1.0000 & -0.0205 & -0.0001 & 0.0004 \\ -0.0205 & 0.9990 & -0.0038 & -0.0083 \\ 0.0002 & 0.0023 & -0.7716 & 0.6345 \\ -0.0003 & -0.0089 & -0.6346 & -0.7716 \end{pmatrix}, \tag{18a}$$

$$\mathbf{M}_{\mathrm{NPT}}^{\mathrm{cc}} = \begin{pmatrix} 1.0000 & -0.0039 & 0.0004 & -0.0017 \\ -0.0038 & 0.9990 & 0.0175 & -0.0705 \\ -0.000 & 0.0001 & 0.9690 & 0.2428 \\ -0.0017 & 0.0726 & -0.2428 & 0.9690 \end{pmatrix},$$
$$\mathbf{M}_{\mathrm{NPT}}^{\mathrm{m}} = \begin{pmatrix} 1.0000 & -0.0060 & 0.0000 & -0.0001 \\ -0.0060 & 0.9990 & -0.0007 & 0.0030 \\ -0.0000 & -0.0001 & 0.9671 & 0.2505 \\ 0.0001 & -0.0031 & -0.2505 & 0.9671 \end{pmatrix}, \tag{18b}$$

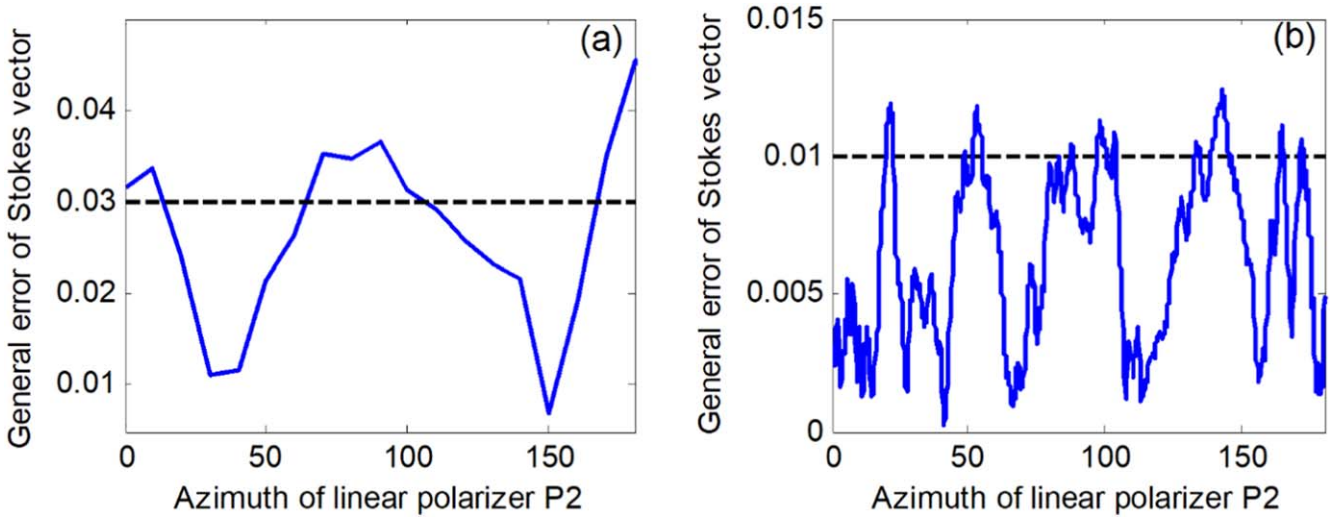

Figure 5. Measured Stokes vector errors, (a) without the proposed method and (b) with the proposed method.

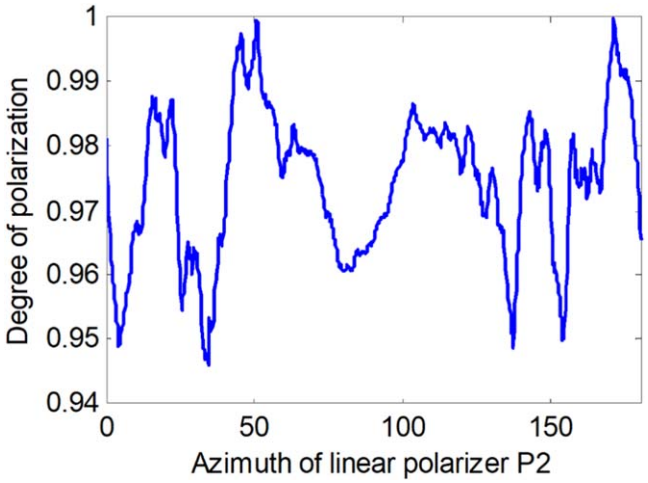

Figure 6. Degree of polarization measurement results using proposed calibration method.

$$\mathbf{M}_{\mathrm{PR}}^{\mathrm{cc}} = \begin{pmatrix} 1.0000 & -0.9969 & -0.0024 & -0.0065 \\ -0.9968 & 0.9999 & 0.0024 & 0.0065 \\ 0.0000 & -0.0004 & 0.1562 & -0.0016 \\ 0.0249 & -0.0260 & 0.0015 & 0.1560 \end{pmatrix},$$

$$\mathbf{M}_{\mathrm{PR}}^{\mathrm{m}} = \begin{pmatrix} 1.0000 & -0.9982 & -0.0151 & -0.0743 \\ -0.9994 & 1.0000 & 0.0149 & 0.0730 \\ 0.0018 & -0.0010 & -0.1224 & -0.0000 \\ -0.0231 & -0.0187 & -0.0008 & -0.1254 \end{pmatrix}, \quad (18c)$$

$$\mathbf{M}_{\mathrm{PT}}^{\mathrm{cc}} = \begin{pmatrix} 1.0000 & -0.9999 & -0.0148 & -0.0011 \\ -0.9999 & 0.9998 & 0.0148 & 0.0011 \\ 0.0000 & 0.0000 & 0.0000 & 0.0000 \\ 0.0164 & -0.0164 & -0.0002 & 0.0000 \end{pmatrix},$$

$$\mathbf{M}_{\mathrm{PT}}^{\mathrm{m}} = \begin{pmatrix} 1.0000 & -0.9983 & -0.0022 & -0.0860 \\ -0.9994 & 0.9960 & 0.0026 & 0.0857 \\ 0.0004 & -0.0013 & 0.0029 & -0.0003 \\ 0.0248 & -0.0255 & 0.0021 & 0.0030 \end{pmatrix}, \quad (18d)$$

where superscript 'c.c.' represents the compensated Mueller matrices, superscript 'm' represents the measured Mueller matrices; subscripts 'NPR' and 'PR' represent the reflection Mueller matrices of the 50:50 (*R*:*T*) NPBS and PBS accordingly, subscripts 'NPT' and 'PT' represent the transmission Mueller matrices of the 50:50 (*R*:*T*) NPBS and PBS similarly.

As shown in equation (18), the differences between the compensated matrices and measured matrices are mainly in the Mueller elements (m_{13}, m_{31}) for the NPBS and (m_{03}, m_{13}) for PBS, which are affected by depolarization seriously as predicted. However, the rest Mueller elements have also changed, indicating that the skew problem of the beam splitter does not only affect CB. The relationship between the tilt angle ϕ and the optical parameter γ is not precise enough. To clearly understand and even formulate the mechanism of skew effects, more comprehensive studies on this problem still need to be carried out in the future.

Different from the previous calibration method which only calibrating the wave plates and linear polarizers and using the Mueller matrix of beam splitters obtained by the MME directly, the Mueller matrices of the beam splitters are obtained by the *in situ* calibration in the proposed calibration method. Then, a comparison between the calibration results of the previous and proposed calibration methods is carried out for verifying the improved accuracy of the instrument by *in situ* calibration of the beam splitters. The system calibration is performed on a well-characterized standard 22 nm SiO_2 thin film on a silicon substrate. The general error of Stokes vector is qualified by equation (19)

$$Dev_{Sto} = \sqrt{\frac{\sum_{i=0}^{3}(S_i - \hat{S}_i)^2}{4}}, \quad (19)$$

where S_i is the ith element of the ideal Stokes vector, $\hat{S}_i$ is the ith element of the calibrated Stokes vector.

As shown in figure 5, the improved calibration reduces the general error of Stokes vector from 3% to 1%. Due to the imperfection in the quart-wave plate C_1, the light before

Table 4 SiO_2 thin film samples with different thickness measured by Stokes polarimeter (SP) and MME.

	10 nm				25 nm			
Samples	ψ (°)	Δ (°)	d (nm)	n	ψ (°)	Δ (°)	d (nm)	n
MME[a]	30.86 ± 0.005	172.65 ± 0.015	11.04 ± 0.003	1.462	31.25 ± 0.005	160.13 ± 0.016	32.53 ± 0.003	1.462
SP[b]	30.77 ± 0.124	173.81 ± 0.175	10.32 ± 0.067	1.470	30.73 ± 0.131	160.77 ± 0.119	31.74 ± 0.175	1.482
Samples	128 nm				1026 nm			
	ψ (°)	Δ (°)	d (nm)	n	ψ (°)	Δ (°)	d (nm)	n
MME	57.42 ± 0.009	193.32 ± 0.030	132.46 ± 0.003	1.462	30.85 ± 0.007	173.75 ± 0.023	1032.92 ± 0.097	1.462
SP	57.17 ± 0.111	194.28 ± 0.463	132.67 ± 0.149	1.462	30.77 ± 0.116	173.49 ± 0.447	1031.55 ± 0.744	1.462

[a] The measurement results reported by MME do not contain the uncertainty of the refractive index n.
[b] The uncertainty of refractive index n of 10 nm, 25 nm, 128 nm and 1026 nm SiO_2 thin film samples are 3.25×10^{-4}, 2.40×10^{-3}, 5.10×10^{-4} and 2.53×10^{-7} respectively.

polarizer P_2 is actually elliptical polarized light instead of right-circular polarized light. So, the intensity of the incident light will change with the polarization state and the error will be larger when the signal-to-noise ratio is relatively small, which may be the reason why the error is slightly greater than 1%, for some polarization states as shown in figure 5(b).

In order to assess the depolarization of the optical system, the degree of the polarization p of the output light can be defined by equation (20). In addition, the relationship between the degree of the polarization of the output light and the azimuth of the linear polarimeter P_2 which is calculated by the proposed calibration method has been shown in figure 6. We can find that the degree of polarization is above 95% and varying with the polarization state of the incident light. Meanwhile, it should be noted that the depolarization is not only caused by the beam splitters, but also due to the standard sample used in calibration or the light reflected back and forth between optical components, and so on

$$p = \sqrt{\frac{S_1^2 + S_2^2 + S_3^2}{S_0^2}}. \tag{20}$$

Finally, the performance of the polarimeter calibrated by the improved calibration method is evaluated by comparing the measured thicknesses of a set of standard SiO_2 thin films with the results reported by a commercial MME. These thin films are measured by the polarimeter when the incident light is set as a linear polarized light oriented at 45°. In table 4, the results reported by both the commercial MME and the house-developed SP are list. These results include the ellipsometric angles (ψ and Δ), the thickness d and the refractive index n for the SiO_2 thin film. Besides, the uncertainties of the results reported by the SP are obtained from 30 repeated measurements and shown in table 4.

As shown in table 4, the results achieved by the SP are in good agreement with the results obtained by the commercial MME. The difference of the ellipsometric angles (ψ, Δ) is about 1°, and the indication errors between the two reports are all within 1 nm, and the differences between the two reported refractive indices are within 1.2%. Meanwhile, the measurement uncertainties are greater than the uncertainties of the MME. The measurement stability of the Stokes polarizer needs to be improved. In general, the experimental results demonstrate that the SP calibrated with the proposed method exhibits the comparable performance as a commercial MME.

5. Conclusions

A characterization method based on the Mueller matrix ellipsometry has been proposed to characterize the beam splitters, with the combination of a calibration process for a house-developed SP. The proposed characterization model enables a decoupled extraction of all the related effective optical parameters so that the Mueller matrix can be rebuilt without any loss of optical information. The improvement of the characterization model is examined by comparing with other existing characterization methods. The average residual errors of Mueller matrices achieved are less than 2×10^{-3} for PBS, and 6×10^{-4} for NPBS, respectively. With the proposed method applied, a six-channel SP with five beam splitters can be delicately calibrated and the general error of Stokes vector can be reduced from 3% to 1%. The experimental results on the thickness measurement of SiO_2 thin film samples show that the performance of the well calibrated SP is comparable to a commercial MME.

Acknowledgments

This work was funded by the National Natural Science Foundation of China (Grant Nos. 51575214, 51525502, 51727809, and 51775217); the National Key Research and Development Plan (Grant No. 2017YFF0204705); the Natural Science Foundation of Hubei Province of China (Grant No. 2018CFA057); and the National Science and Technology Major Project of China (Grant No. 2017ZX02101006-004); the China Postdoctoral Science Foundation (Grant Nos. 2016M602288 and 2017T100546).

ORCID iDs

Hao Jiang https://orcid.org/0000-0003-0561-5058
Xiuguo Chen https://orcid.org/0000-0002-7067-5084
Shiyuan Liu https://orcid.org/0000-0002-0756-1439

References

[1] Wang B, Zhou C, Wang S and Feng J 2007 Polarizing beam splitter of a deep-etched fused-silica grating *Opt. Lett.* **32** 1299–301
[2] Wang W 2009 Wide-angle and broadband nonpolarizing parallel plate beam splitter *Proc. SPIE* **7282** 72821F
[3] Azzam R M A 1985 Beam-splitters for the division-of-amplitude photopolarimeter *J. Mod. Opt.* **32** 1407–12
[4] De A and Azzam R M A 2003 Optimal beam splitters for the division-of-amplitude photopolarimeter *J. Opt. Soc. Am.* A **20** 955–8
[5] Lysenko G A, Krioukov A V, Kachurin Y Y and Pogodaev V V 2006 Accurate measurements at interferometric ellipsometer *Opt. Eng.* **45** 023605
[6] Liu Y-C, Lo Y-L and Liao C-C 2016 Compensation of non-ideal beam splitter polarization distortion effect in Michelson interferometer *Opt. Commun.* **361** 153–61
[7] Pezzaniti J L and Chipman R A 1994 Angular dependence of polarizing beam-splitter cubes *Appl. Opt.* **33** 1916–29
[8] Tyan R-C, Salvekar A A, Chou H-P, Cheng C-C, Scherer A, Sun P-C, Xu F and Fainman Y 1997 Design, fabrication, and characterization of form-birefringent multilayer polarizing beam splitter *J. Opt. Soc. Am.* A **14** 1627–36
[9] Li L and Dobrowolski J 2000 High-performance thin-film polarizing beam splitter operating at angles greater than the critical angle *Appl. Opt.* **39** 2754–71
[10] Elmore D F, Lites B W, Tomczyk S, Skumanich A, Dunn R B, Schuenke J A, Streander K V, Leach T W, Chambellan C and Hull H K 1992 Advanced Stokes polarimeter: a new instrument for solar magnetic field research *Proc. SPIE* **1746** 22–34
[11] Collins P, Redfern R M and Sheehan B 2008 Design, construction and calibration of the Galway astronomical Stokes polarimeter (GASP) *AIP Conf. Proc.* **984** 241

[12] Collins P, Kyne G, Lara D, Redfern M, Shearer A and Sheehan B 2013 The Galway astronomical Stokes polarimeter: an all-Stokes optical polarimeter with ultra-high time resolution *Exp. Astron.* **36** 479–503
[13] Tyo J S, Goldstein D L, Chenault D B and Shaw J A 2006 Review of passive imaging polarimetry for remote sensing applications *Appl. Opt.* **45** 5453–69
[14] Howe J D, Miller M A, Blumer R V, Petty T E, Stevens M A, Teale D M and Smith M H 2000 Polarization sensing for target acquisition and mine detection *Proc. SPIE* **4133** 202–14
[15] Guo X, Wood M and Vitkin A I 2006 Angular measurements of light scattered by turbid chiral media using linear Stokes polarimeter *J. Biomed. Opt.* **11** 041105
[16] Firdous S and Ikram M 2007 Stokes polarimetry for the characterization of bio-materials using liquid crystal variable retarders *Proc. SPIE* **6632** 14
[17] Azzam R M A 1996 Keynote speech: recent developments of division-of-amplitude photopolarimeters *Proc. SPIE* **2873** 1–5
[18] Azzam R M A and Sudradjat F F 2005 Single-layer-coated beam splitters for the division-of-amplitude photopolarimeter *Appl. Opt.* **44** 190–6
[19] Azzam R M A 1982 Division-of-amplitude photopolarimeter (DOAP) for the simultaneous measurement of all four Stokes parameters of light *J. Mod. Opt.* **29** 685–9
[20] Boulbry B, Ramella-Roman J C and Germer T A 2007 Improved method for calibrating a Stokes polarimeter *Appl. Opt.* **46** 8533–41
[21] Compain E, Poirier S and Drevillon B 1999 General and self-consistent method for the calibration of polarization modulators, polarimeters, and Mueller-matrix ellipsometers *Appl. Opt.* **38** 3490–502
[22] Liu J, Zhang C, Zhong Z, Gu H, Chen X, Jiang H and Liu S 2018 Measurement configuration optimization for dynamic metrology using Stokes polarimetry *Meas. Sci. Technol.* **29** 054010
[23] Wang B and Oakberg T C 1999 A new instrument for measuring both the magnitude and angle of low level linear birefringence *Rev. Sci. Instrum.* **70** 3847–54
[24] Lo Y-L and Chen P-C 2010 Characterization on five effective parameters of anisotropic optical material using Stokes parameters—demonstration by a fiber-type polarimeter *Opt. Express* **18** 9133–50
[25] Lo Y-L 2012 Extraction of effective parameters of turbid media utilizing the Mueller matrix approach: study of glucose sensing *J. Biomed. Opt.* **17** 097002
[26] Manhas S, Swami M, Buddhiwant P, Ghosh N, Gupta P and Singh K 2006 Mueller matrix approach for determination of optical rotation in chiral turbid media in backscattering geometry *Opt. Express* **14** 190–202
[27] Liao C-C and Lo Y-L 2013 Extraction of anisotropic parameters of turbid media using hybrid model comprising differential-and decomposition-based Mueller matrices *Opt. Express* **21** 16831–53
[28] Ossikovski R 2011 Differential matrix formalism for depolarizing anisotropic media *Opt. Lett.* **36** 2330–2
[29] Azzam R M A 1978 Propagation of partially polarized light through anisotropic media with or without depolarization: a differential 4×4 matrix calculus *J. Opt. Soc. Am.* **68** 1756–67
[30] Chipman R A 2005 Depolarization index and the average degree of polarization *Appl. Opt.* **44** 2490–5
[31] Azzam R M A and Bashara N M 1987 *Ellipsometry and Polarized Light* (Amsterdam: North-Holland) pp 490–2
[32] Fujiwara H 2007 *Spectroscopic Ellipsometry: Principles and Applications* (Tokyo: Maruzen Co. Ltd) pp 86–7